ETH Library

Evolution-guided engineering of trans-acyltransferase polyketide synthases

Journal Article

Author(s):
Mabesoone, Mathijs F. J.; Leopold-Messer, Stefan; Minas, Hannah A.; Chepkirui, Clara; Chawengrum, Pornsuda; Reiter, Silke; Meoded, Roy A.; Wolf, Sarah; Genz, Ferdinand; Magnus, Nancy; Piechulla, Birgit; Walker, Allison S.; Piel, Jörn

Publication date:
2024-03-21

Permanent link:
https://doi.org/10.3929/ethz-b-000665582

Rights / license:
Creative Commons Attribution 4.0 International

Originally published in:
Science 383(6689), https://doi.org/10.1126/science.adj7621

Funding acknowledgement:
101022873 - PrediKSion: An evolutionary guided and experimentally validated computational pipeline to unravel new polyketide synthase functionality (EC)
742739 - Tailored chemical complexity through evolution-inspired synthetic biology (EC)
185077 - Investigating and utilizing uncultivated bacteria as a rich resource of bioactive natural products (SNF)
197245 - Understanding and exploiting oxidative modifications by modular polyketide synthases (SNF)

This page was generated automatically upon download from the ETH Zurich Research Collection.
For more information, please consult the Terms of use.

TITLE

Evolution-Guided Engineering of *Trans*-Acyltransferase Polyketide Synthases

AUTHORS

Mathijs F.J. Mabesoone[1]†, Stefan Leopold-Messer[1]†, Hannah A. Minas[1]†, Clara Chepkirui[1], Pornsuda Chawengrum[1,2], Silke Reiter[1], Roy A. Meoded[1], Sarah Wolf[1], Ferdinand Genz[1], Nancy Magnus[3], Birgit Piechulla[3], Allison S. Walker[4, 5, 6], Jörn Piel[1, 7]*

AFFILIATIONS

[1]Institute of Microbiology, Eidgenössische Technische Hochschule (ETH) Zürich, Vladimir-Prelog-Weg 4, 8093 Zürich, Switzerland.

[2]Chemical Biology Program, Chulabhorn Graduate Institute, Chulabhorn Royal Academy, Bangkok 10210, Thailand.

[3]Institute for Biological Sciences, University of Rostock, Albert-Einstein-Straße 3, 18059 Rostock, Germany.

[4]Department of Biological Chemistry and Molecular Pharmacology, Harvard Medical School, 240 Longwood Avenue, Boston, Massachusetts 02115, United States.

[5]Department of Chemistry, Vanderbilt University, 1234 Stevenson Center Lane, Nashville, Tennessee 37240, United States.

[6]Department of Biological Sciences, Vanderbilt University, 465 21st Avenue S, Nashville, Tennesee 37232, United States.

[7]Lead contact

†These authors contributed equally

*E-mail: jpiel@ethz.ch

Further information and requests for resources and reagents should be directed to and will be fulfilled by the lead contact, Jörn Piel (jpiel@ethz.ch).

ABSTRACT

Bacterial multimodular polyketide synthases (PKSs) are giant enzymes that generate a wide range of therapeutically important but synthetically challenging natural products. Diversification of polyketide structures can be achieved by engineering these enzymes. However, notwithstanding successes made with textbook, *cis*-acyltransferase (*cis*-AT) PKSs, tailoring such large assembly lines remains challenging. Unlike textbook PKSs, *trans*-AT PKSs feature an extraordinary diversity of PKS modules and commonly evolve to form hybrid PKSs. Here, we analyze amino acid coevolution to identify a common module site that yields functional PKSs. We use this site to insert and delete diverse PKS parts and create 22 engineered *trans*-AT PKSs from various pathways and in two bacterial producers. The high success rates of our engineering approach highlight the broader applicability to generate complex designer polyketides.

ONE-SENTENCE SUMMARY

Evolutionary insights enable the engineered biosynthesis of designer polyketides, an important class of bioactive natural products.

MAIN TEXT

Bacteria are a rich source of bioactive natural products, many of which have found pharmacological applications (*1*). Among the most therapeutically useful compounds are complex polyketides produced by large megaenzymes termed polyketide synthases (PKSs) (*2–4*). These assembly line-like proteins are composed of multiple modules, each introducing a specific part of the final structure. Biosynthesis is achieved by stepwise incorporation and modification of small acyl-CoA-derived building blocks. Textbook multimodular PKSs, coined *cis*-AT PKSs, largely contain modules employing fatty acid synthase-type biochemistry. A minimal module consists of an acyl carrier protein (ACP) domain tethering the polyketide intermediate, a ketosynthase (KS) domain catalyzing the chain elongation, and an acyl transferase (AT) domain selecting the building blocks. Optional additional modifications at the β-carbon, such as reductions by ketoreductases (KR) or dehydrations by dehydratases (DH), diversify the polyketide scaffold to generate chemical complexity. The sequence of modules is represented in the chemical structure of the final product – a phenomenon termed the collinearity principle. This correspondence at the protein and chemical level has inspired the vision to create designer PKSs from module parts that produce synthetically challenging polyketides in a predictable fashion (*5*). Efforts towards engineering have been successful for the erythromycin PKS and other model systems (*6–8*), yet design rules that enable combinatorial biosynthesis with high success rates remain elusive (*9*). The observation that KSs from *cis*-AT systems typically form distinct clades with other KSs from the same cluster (*10*) suggests the formation of natural hybrids by recombination is rare in *cis*-AT PKSs, which might represent an intrinsic challenge to engineering of this family of PKSs.

A second large family of bacterial multimodular PKSs, termed *trans*-AT PKSs, differ from *cis*-AT assembly lines (*11*). They commonly contain modules catalyzing non-fatty acid synthase-type reactions, such as halogenation (*12*, *13*), formation of diverse heterocycles (*14–16*), oxygen insertion (*17*, *18*), α-hydroxylation (*13*), and β-branching (*15*, *19*). This unparalleled biochemical diversity provides a vast combinatorial space to diversify polyketide structures in a modular fashion. *Trans*-AT PKSs evolve via widespread recombination between biosynthetic gene clusters (BGCs) to form mosaic-like natural hybrids (*20*). A common recombination site is located at a region corresponding to the C-terminus of KS domains (*21*, *22*), i.e., KSs coevolve with modifying domains located directly upstream (*20*, *23*). Together, the apparent natural combinatorial evolution of *trans*-AT PKSs and their expanded chemical repertoire make this class of enzymes highly attractive for engineering efforts. Guidelines to engineer these megaenzymes remain, however, unclear from the few reported modified *trans*-AT PKSs (*24*, *25*). Here, we leverage insights obtained from natural *trans*-AT PKS evolution to uncover a fusion site that allows construction of diverse engineered, large PKS assembly lines in several organisms.

Fusions at a conserved NAHVILEE motif result in stalled intermediates

In a first attempt to identify the natural recombination sites in *trans*-AT PKSs, we extracted 821 KS sequences with their adjacent up- and downstream regions from our in-house database of

annotated *trans*-AT PKS biosynthetic gene clusters (*20*, *26*). A multiple sequence alignment showed a conserved NAHVILEE motif near the C-terminus of KSs (Fig. S1). In many natural *trans*-AT PKS hybrids with shared module series (*21*, *22*), we observed that pairwise sequence similarity dropped off behind the NAHVILEE motif of the terminal, shared module. However, a putative recombination site could not be precisely localized within a ca. 100 amino acid region due to high sequence divergences even among architecturally closely related PKS hybrids. Since the NAHVILEE motif was also reported as a functional fusion site to yield functional *cis*-AT PKS chimeras (*27*, *28*), we explored its utility for *trans*-AT engineering using the bacillaene (*pks*) biosynthetic gene cluster from *Bacillus subtilis* (*29*, *30*). Four chimeric PKSs were generated by genomic integration, resulting in PKSs with non-native terminal modules (Figs. S1-6, see Supplementary Information for additional details). However, instead of full-length polyketides, we detected products that resulted from hydrolytic release of stalled intermediates just before the fusion point. The data suggested that none of the chimeras was functional and that the NAHVILEE site is not suitable for engineering in this PKS.

Statistical coupling analysis suggests the LPTYPFx_5W motif as potential recombination site

To infer the site at which *trans*-AT PKSs potentially recombine, we analyzed amino acid coevolution with statistical coupling analysis (SCA) (*31*, *32*). This method analyzes covariance of amino acids in multiple sequence alignments and identifies global networks of coevolving residues. We reasoned that this method might reveal structurally or functionally interconnected networks of amino acid residues that might be sensitive to disruption by engineering (Fig. 1A). Due to dynamic processes during polyketide elongation as well as lateral interactions between assembly lines that create a multitude of domain contacts (*33*, *34*), such residue interactions remain obscure when using the available structural snapshots of *trans*-AT PKS components (*35*, *36*). As such, we hypothesized that SCA might uncover engineering sites at boundaries between independent networks of coevolving residues that minimally disrupt evolutionary conserved interactions in *trans*-AT PKSs and thereby enable engineering of productive chimeric *trans*-AT PKSs. For analysis, we extracted protein sequences that encompass the KS domain and commonly occurring neighboring regions from manually collected *trans*-AT PKSs and *trans*-AT PKSs deposited in the antiSMASH database (Fig. S9) (*37*) and analyzed sequence alignments with SCA (see Supplementary Materials). The amino acid covariance in the alignments of the extracted motifs reveals coevolution within each modifying domain (e.g., KS and KR, Figs. 1B, S10-12). In addition, covariance between KS domains and upstream modifying domains is also apparent, which is in line with the previous observation that KSs clade according to the polyketide modifications introduced by these upstream modifying domains (Figs. S10-12) (*20*, *23*). We additionally observed coevolution of residues within the KS and a C-terminal region termed flanking subdomain (FSD) (Figs. 1B, S10-12). Although the precise function of the FSD is unclear, it has been found to mediate lateral interactions between PKSs to form higher-order, supramolecular PKS assemblies (*33*, *36*, *38–40*), suggesting this subdomain plays an important role in the organizational dynamics of polyketide biosynthesis.

To test whether this coevolution between KS and FSD is significant, we deconvoluted the amino acid covariance and extracted networks of statistically significantly coevolving positions. The most

significant of the amino acid networks, coined sectors, has been associated with conserved residues and general enzyme stability (*41*), whereas other significant sectors that contain less-conserved residues are associated with more specialized enzyme functionality (*41*, *42*). We consistently found that the LPTYPFx_5W motif at the FSD C-terminus acts as boundary between sectors containing lesser-conserved residues that are presumably involved in enzyme functionality (Figs. 1C, D, S13). This suggested that the LPTYPFx_5W motif, which also occurs in *cis*-AT PKSs downstream of the AT domain and has been successfully used in AT swapping experiments in *cis*-AT PKSs (*43*, *44*), separates evolutionarily autonomous parts in *trans*-AT PKSs. In line with terminology from NRPS engineering (*45*), we use the term "exchange units" for these evolutionarily autonomous parts that contain various domains (*25*, *34*, *46*), while "module" refers to biochemically functional KS-to-ACP sections (Fig. 1A).

A *Serratia plymuthica* platform for PKS engineering

To experimentally assess whether the computationally suggested LPTYPFx_5W motif can serve as an artificial fusion site, we developed a screening platform using the oocydin BGC in the genetically tractable bacterium *Serratia plymuthica* 4Rx13 (henceforth termed *S. plymuthica*) (*13*, *17*). The oocydin *trans*-AT PKS contains biochemically diverse modules including a halogenation module that catalyzes chlorination during polyketide chain elongation (*13*, *47*). This module comprises a heterodimer of the *trans*-acting Fe(II)/α-ketoglutarate-dependent halogenase OocP and the auxiliary protein OocQ (Figs. 2A, S14). By using the chlorination module at the engineering interface, we hoped to introduce a characteristic chlorine isotope tag into hybrid polyketides that would facilitate their mass spectrometric detection in bacterial extracts (*47*).

High-performance liquid chromatography coupled to mass spectrometry (HPLC-MS) analysis of culture extracts of *S. plymuthica* Δ*oocQR*, a mutant lacking *oocQ* and the downstream PKS gene *oocR*, showed that chlorination of polyketide intermediates was indeed abolished (Fig. 2C). We next supplemented *oocQ* to *S. plymuthica* Δ*oocQR* on a plasmid encoding *oocQ* and *oocR* up to the LPTYPFx_5W motif of the second KS of OocR (*pBAD-oocQR*) (Fig. 2B, top). Besides restoring oocydin production (Fig. S30), supplementation of *oocQR* also resulted in the production of a compound with an *m/z* value corresponding to compound **1** (Figs. 2C-E), the free acid of the putative polyketide intermediate at the OocR ACP domain (*13*), thereby confirming restored chlorination by supplementation of *oocQ*. With the aim to facilitate processivity of the truncated assembly line, we next appended the terminal ACP-C didomain of OocS to the truncated OocR. This didomain natively offloads the polyketide intermediate by catalyzing macrolactonization (*13*). Extracts resulted in larger amounts of a product with an additional C_2 extension. NMR-based structural elucidation after HPLC-MS-guided fractionation confirmed the macrolactone structure of **2** (Figs. 2C, D, F, S17-21). *S. plymuthica* Δ*oocQR* thus provides a platform for introducing engineered *oocR* mutants to assess guidelines for *trans*-AT PKS engineering (Fig. 2G).

Introducing foreign domains after the LPTYPFx_5W motif yields functional chimeric PKSs

Having generated a functional engineered PKS with native *ooc* parts, we next explored the compatibility of the LPTYPFx_5W site with a foreign component. To minimize the number of non-native interactions, we introduced a single fusion site by joining the truncated *oocR* to the terminus

of the psymberin (*psy*) BGC from an uncultivated bacterium (*21*). The *psy* region encodes the domain series ACP-KS-DUF-DH-ACP (DUF: domain of unknown function), and an offloading thioesterase (TE) domain that jointly catalyze β-keto extension and δ-lactone formation (Fig. 3A). The *psy* KS natively accepts a β-ketoacyl intermediate (*21*), as would be produced by the upstream minimal ACP-KS domain series that is the result of the PKS fusion (*13*). As a control experiment, we constructed a PKS with the same domains, but the fusion point located at the NAHVILEE motif of the OocR KS. HPLC-MS analysis of medium extracts showed that only the LPTYPFx_5W-fused chimera suggested by SCA produces a chlorinated compound with an *m/z* value of 511.1729, corresponding to the expected, doubly extended product **3** (Figs. 3B, C), whereas the NAHVILEE-fused chimera yielded offloaded intermediates **1** and **2**. HPLC-guided purification and structural elucidation confirmed **3** as a pyrone resulting from two keto extensions and δ-lactone formation (Figs. 3D, S22-26).

Having established the utility of the LPTYPx_5W site for new PKS termini, we next aimed to insert foreign domains between domains of the *ooc* assembly line. For this, we placed an exchange unit containing a β-ketoacyl-accepting minimal ACP-KS12 domain series from the lobatamide (*lbm*) PKS of *Gynuella sunshinyii* (*18*) between the truncated OocR and the OocS ACP C terminus (Fig. 3E). If functional, this PKS would catalyze two terminal keto extensions as for the *psy* construct. In addition to the SCA-conform LPTYPx_5W double fusion, we prepared three control constructs with one or both *lbm* fusion sites exchanged to the NAHVILEE motif (Figs. 3E, F). HPLC-MS analysis showed that fusion the LPTYPx_5W motif at both sites led to notable production of **3**, whereas fusion at the NAHVILEE motif at any of the two sites primarily showed stalled biosynthesis, indicated by only trace amounts of **3**. Mutants employing a fusion site upstream of the OocR KS12, which was shown to yield productive truncated disorazol PKSs (*24*), were not productive (Fig. S15). We thus concluded that the LPTYPx_5W motif provides an engineering site for chimeric *trans*-AT PKSs and used this fusion site in our further experiments.

A wide range of exchange units with minimal ACP-KS domain series is tolerated

Excised KS domains can accept and elongate substrates *in vitro* that differ from the natively encountered polyketide intermediate, albeit at lower rates (*14*). This promiscuity suggests that the β-ketoacyl thioesters presented by the truncated OocR PKS can be extended by foreign KS domains that natively elongate different substrates. To test this hypothesis, we constructed five chimeric PKSs with ACP-KS inserts that naturally process reduced intermediates (Figs. 3G, H). As above, foreign domains were located between the truncated OocR and $OocS_C$. Two of these chimeric PKSs, containing exchange units harboring *lbm* KS11 and *pks* KS5 (*48*), were excised from larger, dehydrating domain series, whereas the remaining three, harboring KS10 and KS13 from the tartrolon BGC (*tar*) (*20*) and KS13 from the lacunalide (*lcn*) BGC, both from *G. sunshinyii* (*26*), occur naturally in a minimal KS-ACP architecture. We observed production of **3** for all mutants (Fig. 3H). However, 3 to 50-fold lower HPLC-MS intensities suggested impaired processivity of the chimeric assembly lines, likely due to decreased rates of elongation. This hypothesis is additionally supported by the increased intensity of signals attributable to hydrolysis products of stalled intermediates with masses near-identical to the mass of **3**, but slightly shorter retention time (Figs.

3H, S16). While these lower intensities suggest that matching KSs increase titers in PKS engineering, the notion that KS specificity might be important for engineering *trans*-AT PKSs (*49*, *50*) seems not to be stringent. Encouraged by the six functional chimeras containing exchange units of foreign domain series from interior protein regions, we also tested ACP-KS domain series from the N-termini of PKS proteins at the same engineering site. A chimeric PKS containing *lcn* KS24 with its upstream tandem ACP also produced **3**, albeit at considerably lower titers than those observed for constructs incorporating domain series excised from internal modules (Fig. 3J). Unexpectedly, **3** was also produced by a chimera harboring the ACP-less KS1 from the start of the entire *lcn* assembly line, i.e., containing a tandem KS (Fig. 3I). Collectively, these data show that *trans*-AT PKS engineering at the LPTYPFx_5W motif enables incorporation of minimalACP-KS domain series from diverse biosynthetic context with variable processivity.

Chimeric assembly lines with foreign β-keto-modifying domain series

Having shown that our engineering strategy allows for insertion of exchange units of diverse minimal ACP-KS domain series into a PKS, we interrogated the engineering scope for exchange units of domain series that contain additional modifying domains. First, we inserted reducing exchange units comprising KR, ACP, and KS domains into the test site (Fig. 4A). The selected exchange units contain *tar* KS11, *gyn* KS3, and *lcn* KS6 from the lacunalide, gynuellalide, and tartrolon pathways, respectively. For the *gyn* and *tar* chimeras, HPLC-MS analysis showed a chlorinated compound with *m/z* values corresponding to the singly extended and reduced product **4** (Figs. 4A-D). Lastly, we inserted exchange units of dehydrating domain series incorporating *lbm* KS9, *lbm* KS11, and *pks* KS5 with the architecture DH-KR-ACP-KS into OocR (Fig. 4E). The resulting mutants produced two chlorinated, isobaric compounds eluting around 14.5 minutes, suggesting the presence of *E*- and *Z*-isomers of the singly extended and dehydrated polyketide **5** (Figs. 4F-H). Although the low titers precluded isolation of **4** and **5**, the presence of both ammonium and sodium adducts of these compounds and their absence in *S. plymuthica* Δ*oocQR* extracts (Figs. 4D, H, S28) suggest that the engineering strategy also allows for the incorporation of exchange units that not only elongate but also modify the polyketide intermediate.

Engineering at LPTYPFx_5W motifs enables biosynthesis of truncated lacunalides

We further tested the generality of the engineering strategy by applying it to a different bacterial host and assembly line, i.e., the lacunalide PKS of *G. sunshinyii* YC6258 (Fig. 5A). Using the statistically identified LPTYPFx_5W motif, we deleted exchange units of *lcn* modules 14 and 15 containing a DH-KR-ACP-KS-KR-ACP-KS domain series, to produce the mutant *G. sunshinyii* YC6258 Δ*lcn14-15* (Figs. 5A, B). In this design, we specifically aimed to match the α-δ regions of the putative polyketide intermediate with the moiety that is naturally accepted by the downstream KS (Fig. S54). Based on biosynthetic logic, a functional engineered PKS would not generate lacunalides A, **6**, and B, **7**, but instead the spliced lacunalides **8** and **9** (Figs. 5B, C). In line with this hypothesis, MS features corresponding to **8** and **9** were only observed in culture extracts of *G. sunshinyii* YC6258 Δ*lcn14-15*, whereas production of **6** and **7** was completely abolished in this mutant. HPLC purification and combined NMR and MS analysis confirmed the structure of truncated lacunalides **8** and **9** (Figs. S62-79). The stable genomic integration of the *lcn* PKSs

truncation allows combination of multiple such modifications. While taking the above-mentioned design principles into account, we then deleted three further exchange unit series in the *lcn* PKS, covering modules 21-22; 20-23 and 17-24 (Fig. 5A) from the wild-type producer as well as from the mutant *G. sunshinyii* YC6258 Δ*lcn14-15*. HPLC-MS analysis of culture extracts of the respective mutants revealed distinct MS features corresponding to truncated lacunalides **10**-**21** (Fig. 5B). To verify the processivity of all members of this engineered PKS library, we isolated compounds from each *G. sunshinyii* mutant and determined the structure by NMR (Figs. 5B, S80-121). Isolated yields of lacunalide A analogues **8**, **10**, **12** and **20** (0.4-0.7 mg/mL) and lacunalide B analogues **9**, **11** and **21** (0.04-0.21 mg/L) were comparable to yields of the parent lacunalide A (0.7 mg/L) and lacunalide B (0.15 mg/L) (*51*), while the other metabolites were isolated with reduced yields (0.03-0.26 mg/L) (Table S17). Cytotoxicity assays against Henrietta Lacks (HeLa) cervical cancer cells furthermore showcase the utility of our engineering strategy in elucidating structure-activity relationships in synthetically challenging polyketides (Fig. S122). In summary, the seven constructed mutants produced at least 12 different new compounds. As such, these results show that the engineering strategy not only enables introduction of foreign domains into *trans*-AT PKS, but also enables the reductive combinatorial biosynthesis of lacunalide congeners.

Conclusion

We demonstrate that evolution-guided engineering of *trans*-AT PKSs at the FSD LPTYPFx_5W motif provides a useful strategy to construct functional chimeric and truncated complex assembly lines. We show its broad applicability by successfully engineering 22 large, chimeric assembly lines comprising parts from diverse PKSs and using two host organisms and study the bioactivity of several engineered metabolites. The discovery of this engineering principle, in combination with the exceptional biochemical diversity of *trans*-AT PKS modules, offers potential for combinatorial biosynthesis of *de novo* designed, synthetically challenging polyketides including structure-activity relationship studies and drug improvement, pharmacophore discovery and introduction, and the biotechnological production of stereochemically complex fine chemicals.

Acknowledgements

We acknowledge Eric Helfrich and Kira Weissman for helpful discussions and Sarolt Magyari for providing the pBAD vector. The pFusA vector was donated by Adam Bogdanove and Daniel Voytas.

Funding: J.P. acknowledges funding from the European Research Council under the European Union's Horizon 2020 programme (742739, SynPlex), the Gordon and Betty Moore Foundation (https://doi.org/10.37807/GBMF9204), and to the Swiss National Science Foundation (205320_185077 and 205321L_197245). M.F.J.M. acknowledges funding from the European Union's Horizon 2020 research and innovation programme under the Marie Skłodowska-Curie grant agreement no. 101022873. P.C. was supported by the Royal Golden Jubilee Ph.D. program, the National Research Council of Thailand (NRCT5-RGJ63023-176). A.W. acknowlegedes funding from the National Institutes of Health, grant number R35 GM146987.

DATA AND MATERIALS AVAILABILITY

All data, scripts and plasmid maps that support the claims in this manuscript are available on the Zenodo repository (https://doi.org/10.5281/zenodo.8146702) (*52*). Scripts for SCA and HPLC-MS analysis are also available at www.github.com/mathijs-m/PKS_engineering_SCA and www.github.com/mathijs-m/Engineered_PKS_MS_analysis, respectively.

SUPPLEMENTARY MATERIALS

Experimental procedures
Bioinformatic procedures
Design and analysis of chimeric bacillaene *trans*-AT PKSs in *B. subtilis*
Tables S1 to S19
Figs. S1 to S122
MDAR Reproducibility Checklist

AUTHOR CONTRIBUTIONS

Conceptualization: H.A.M., S.L.M., M.F.J.M, S.R., R.A.M., J.P.
Methodology: H.A.M., M.F.J.M, S.L.M., J.P.
Software: M.F.J.M., A.W.
Formal Analysis: M.F.J.M., H.A.M., S.L.M.
Investigation: M.F.J.M., H.A.M., S.L.M., C.C., S.R., P.C., S.W., R.A.M., F.G.
Resources: N.M., B.P.
Writing: M.F.J.M, H.A.M., S.L.M., J.P.
Funding Acquisition: M.F.J.M., J.P.
Supervision: J.P.

DECLARATION OF INTEREST

The authors declare no competing interests.

License information: Copyright © 2024 the authors, some rights reserved; exclusive licensee American Association for the Advancement of Science. No claim to original US government works. https://www.science.org/about/science-licenses-journal-article-reuse

REFERENCES AND NOTES

1. D. J. Newman, G. M. Cragg, Natural Products as Sources of New Drugs over the Nearly Four Decades from 01/1981 to 09/2019. *J. Nat. Prod.* **83**, 770–803 (2020).

2. J. Staunton, K. J. Weissman, Polyketide biosynthesis: a millennium review. *Nat. Prod. Rep.* **18**, 380–416 (2001).

3. T. Robbins, Y.-C. Liu, D. E. Cane, C. Khosla, Structure and mechanism of assembly line polyketide synthases. *Curr. Opin. Struct. Biol.* **41**, 10–18 (2016).

4. M. Grininger, Enzymology of assembly line synthesis by modular polyketide synthases. *Nat. Chem. Biol.* **19**, 401–415 (2023).

5. S. Donadio, M. Staver, J. McAlpine, S. Swanson, L. Katz, Modular organization of genes required for

complex polyketide biosynthesis. *Science*. **252**, 675–679 (1991).

6. J.-M. Massicard, C. Soligot, K. J. Weissman, C. Jacob, Manipulating polyketide stereochemistry by exchange of polyketide synthase modules. *Chem. Commun.* **56**, 12749–12752 (2020).

7. G. Zhai, Y. Zhu, G. Sun, F. F. Zhou, Y. Y. Sun, Z. Hong, C. Dong, P. F. Leadlay, K. Hong, Z. Deng, F. F. Zhou, Y. Y. Sun, Insights into azalomycin F assembly-line contribute to evolution-guided polyketide synthase engineering and identification of intermodular recognition. *Nat. Commun.* **14**, 612 (2023).

8. M. Klaus, M. Grininger, Engineering strategies for rational polyketide synthase design. *Nat. Prod. Rep.* **35**, 1070–1081 (2018).

9. K. J. Weissman, Genetic engineering of modular PKSs: from combinatorial biosynthesis to synthetic biology. *Nat. Prod. Rep.* **33**, 203–230 (2016).

10. A. Nivina, K. P. Yuet, J. Hsu, C. Khosla, Evolution and Diversity of Assembly-Line Polyketide Synthases. *Chem. Rev.* **119**, 12524–12547 (2019).

11. E. J. N. Helfrich, J. Piel, Biosynthesis of polyketides by trans-AT polyketide synthases. *Nat. Prod. Rep.* **33**, 231–316 (2016).

12. L. Gu, B. Wang, A. Kulkarni, T. W. Geders, R. V. Grindberg, L. Gerwick, K. Håkansson, P. Wipf, J. L. Smith, W. H. Gerwick, D. H. Sherman, Metamorphic enzyme assembly in polyketide diversification. *Nature*. **459**, 731–735 (2009).

13. F. Hemmerling, R. A. Meoded, A. E. Fraley, H. A. Minas, C. L. Dieterich, M. Rust, R. Ueoka, K. Jensen, E. J. N. Helfrich, C. Bergande, M. Biedermann, N. Magnus, B. Piechulla, J. Piel, Modular Halogenation, α-Hydroxylation, and Acylation by a Remarkably Versatile Polyketide Synthase. *Angew. Chem. Int. Ed.* **61**, e202116614 (2022).

14. M. Jenner, S. Frank, A. Kampa, C. Kohlhaas, P. Pöplau, G. S. Briggs, J. Piel, N. J. Oldham, Substrate Specificity in Ketosynthase Domains from trans-AT Polyketide Synthases. *Angew. Chem. Int. Ed.* **52**, 1143–1147 (2013).

15. T. Bretschneider, J. B. Heim, D. Heine, R. Winkler, B. Busch, B. Kusebauch, T. Stehle, G. Zocher, C. Hertweck, Vinylogous chain branching catalysed by a dedicated polyketide synthase module. *Nature*. **502**, 124–128 (2013).

16. S. Meng, A. D. Steele, W. Yan, G. Pan, E. Kalkreuter, Y.-C. Liu, Z. Xu, B. Shen, Thiocysteine lyases as polyketide synthase domains installing hydropersulfide into natural products and a hydropersulfide methyltransferase. *Nat. Commun.* **12**, 5672 (2021).

17. R. A. Meoded, R. Ueoka, E. J. N. Helfrich, K. Jensen, N. Magnus, B. Piechulla, J. Piel, A Polyketide Synthase Component for Oxygen Insertion into Polyketide Backbones. *Angew. Chem. Int. Ed.* **57**, 11644–11648 (2018).

18. R. Ueoka, R. A. Meoded, A. Gran-Scheuch, A. Bhushan, M. W. Fraaije, J. Piel, Genome Mining of Oxidation Modules in trans-Acyltransferase Polyketide Synthases Reveals a Culturable Source for Lobatamides. *Angew. Chem. Int. Ed.* **59**, 7761–7765 (2020).

19. A. E. Fraley, C. L. Dieterich, M. F. J. Mabesoone, H. A. Minas, R. A. Meoded, F. Hemmerling, J. Piel, Structure of a Promiscuous Thioesterase Domain Responsible for Branching Acylation in Polyketide Biosynthesis. *Angew. Chem. Int. Ed.* **61**, e202206385 (2022).

20. E. J. N. Helfrich, R. Ueoka, A. Dolev, M. Rust, R. A. Meoded, A. Bhushan, G. Califano, R. Costa, M. Gugger, C. Steinbeck, P. Moreno, J. Piel, Automated structure prediction of trans-acyltransferase polyketide synthase products. *Nat. Chem. Biol.* **15**, 813–821 (2019).

21. K. M. Fisch, C. Gurgui, N. Heycke, S. A. van der Sar, S. A. Anderson, V. L. Webb, S. Taudien, M. Platzer, B. K. Rubio, S. J. Robinson, P. Crews, J. Piel, Polyketide assembly lines of uncultivated sponge symbionts from structure-based gene targeting. *Nat. Chem. Biol.* **5**, 494–501 (2009).

22. R. Ueoka, A. R. Uria, S. Reiter, T. Mori, P. Karbaum, E. E. Peters, E. J. N. Helfrich, B. I. Morinaka, M. Gugger, H. Takeyama, S. Matsunaga, J. Piel, Metabolic and evolutionary origin of actin-binding polyketides from diverse organisms. *Nat. Chem. Biol.* **11**, 705–712 (2015).

23. T. Nguyen, K. Ishida, H. Jenke-Kodama, E. Dittmann, C. Gurgui, T. Hochmuth, S. Taudien, M. Platzer, C. Hertweck, J. Piel, Exploiting the mosaic structure of trans-acyltransferase polyketide synthases for natural product discovery and pathway dissection. *Nat. Biotechnol.* **26**, 225–233 (2008).

24. Z.-J. Wang, X. Liu, H. Zhou, Y. Liu, Q. Tu, L. Huo, F. Yan, R. Müller, Y. Zhang, X. Xu, Engineered Biosynthesis of Complex Disorazol Polyketides in a Streamlined Burkholderia thailandensis. *ACS Synth. Biol.* **12**, 971–977 (2023).

25. M. Till, P. R. Race, Progress challenges and opportunities for the re-engineering of trans-AT polyketide synthases. *Biotechnol. Lett.* **36**, 877–888 (2014).

26. E. J. N. Helfrich, R. Ueoka, M. G. Chevrette, F. Hemmerling, X. Lu, S. Leopold-Messer, H. A. Minas, A. Y. Burch, S. E. Lindow, J. Piel, M. H. Medema, Evolution of combinatorial diversity in trans-acyltransferase polyketide synthase assembly lines across bacteria. *Nat. Commun.* **12**, 1422 (2021).

27. Y. Sugimoto, K. Ishida, N. Traitcheva, B. Busch, H.-M. Dahse, C. Hertweck, Freedom and Constraint in Engineered Noncolinear Polyketide Assembly Lines. *Chem. Biol.* **22**, 229–240 (2015).

28. H. Peng, K. Ishida, Y. Sugimoto, H. Jenke-Kodama, C. Hertweck, Emulating evolutionary processes to morph aureothin-type modular polyketide synthases and associated oxygenases. *Nat. Commun.* **10**, 3918 (2019).

29. A. M. Albertini, T. Caramori, F. Scoffone, C. Scotti, A. Galizzi, Sequence around the 159 region of the Bacillus subtilis genome: the pksX locus spans 33·6 kb. *Microbiology*. **141**, 299–309 (1995).

30. R. A. Butcher, F. C. Schroeder, M. A. Fischbach, P. D. Straight, R. Kolter, C. T. Walsh, J. Clardy, The identification of bacillaene, the product of the PksX megacomplex in Bacillus subtilis. *Proc. Natl. Acad. Sci.* **104**, 1506–1509 (2007).

31. S. W. W. Lockless, R. Ranganathan, Evolutionarily Conserved Pathways of Energetic Connectivity in Protein Families. *Science*. **286**, 295–299 (1999).

32. O. Rivoire, K. A. Reynolds, R. Ranganathan, Evolution-Based Functional Decomposition of Proteins. *PLOS Comput. Biol.* **12**, e1004817 (2016).

33. D. C. Gay, D. T. Wagner, J. L. Meinke, C. E. Zogzas, G. R. Gay, A. T. Keatinge-Clay, The LINKS motif zippers trans-acyltransferase polyketide synthase assembly lines into a biosynthetic megacomplex. *J. Struct. Biol.* **193**, 196–205 (2016).

34. S. Kosol, M. Jenner, J. R. Lewandowski, G. L. Challis, Protein–protein interactions in trans-AT polyketide synthases. *Nat. Prod. Rep.* **35**, 1097–1109 (2018).

35. A. Miyanaga, R. Ouchi, F. Ishikawa, E. Goto, G. Tanabe, F. Kudo, T. Eguchi, Structural Basis of Protein–Protein Interactions between a trans-Acting Acyltransferase and Acyl Carrier Protein in Polyketide Disorazole Biosynthesis. *J. Am. Chem. Soc.* **140**, 7970–7978 (2018).

36. Y. U. Tittes, D. A. Herbst, S. F. X. Martin, H. Munoz-Hernandez, R. P. Jakob, T. Maier, The structure of a polyketide synthase bimodule core. *Sci. Adv.* **8** (2022), doi:10.1126/sciadv.abo6918.

37. K. Blin, S. Shaw, S. A. Kautsar, M. H. Medema, T. Weber, The antiSMASH database version 3: increased taxonomic coverage and new query features for modular enzymes. *Nucleic Acids Res.* **49**, D639–D643 (2021).

38. D. C. Gay, G. Gay, A. J. Axelrod, M. Jenner, C. Kohlhaas, A. Kampa, N. J. Oldham, J. Piel, A. T. Keatinge-Clay, A Close Look at a Ketosynthase from a Trans-Acyltransferase Modular Polyketide Synthase. *Structure*. **22**, 444–451 (2014).

39. E. M. Musiol, T. Weber, Discrete acyltransferases involved in polyketide biosynthesis. *Medchemcomm*. **3**, 871 (2012).

40. Z. D. Aron, P. D. Fortin, C. T. Calderone, C. T. Walsh, FenF: Servicing the Mycosubtilin Synthetase Assembly Linein trans. *ChemBioChem*. **8**, 613–616 (2007).

41. T. Teşileanu, L. J. Colwell, S. Leibler, Protein Sectors: Statistical Coupling Analysis versus Conservation. *PLOS Comput. Biol.* **11**, e1004091 (2015).

42. R. N. McLaughlin Jr, F. J. Poelwijk, A. Raman, W. S. Gosal, R. Ranganathan, The spatial architecture of protein function and adaptation. *Nature*. **491**, 138–142 (2012).

43. S. Yuzawa, K. Deng, G. Wang, E. E. K. Baidoo, T. R. Northen, P. D. Adams, L. Katz, J. D. Keasling, Comprehensive in Vitro Analysis of Acyltransferase Domain Exchanges in Modular Polyketide Synthases and Its Application for Short-Chain Ketone Production. *ACS Synth. Biol.* **6**, 139–147 (2017).

44. E. Englund, M. Schmidt, A. A. Nava, A. Lechner, K. Deng, R. Jocic, Y. Lin, J. Roberts, V. T. Benites, R. Kakumanu, J. W. Gin, Y. Chen, Y. Liu, C. J. Petzold, E. E. K. Baidoo, T. R. Northen, P. D. Adams, L. Katz, S. Yuzawa, J. D. Keasling, Expanding Extender Substrate Selection for Unnatural Polyketide Biosynthesis by Acyltransferase Domain Exchange within a Modular Polyketide Synthase. *J. Am. Chem. Soc.* **145**, 8822–8832 (2023).

45. K. A. J. Bozhüyük, A. Linck, A. Tietze, J. Kranz, F. Wesche, S. Nowak, F. Fleischhacker, Y.-N. Shi, P. Grün, H. B. Bode, Modification and de novo design of non-ribosomal peptide synthetases using specific assembly points within condensation domains. *Nat. Chem.* **11**, 653–661 (2019).

46. G.-L. Tang, Y.-Q. Cheng, B. Shen, Leinamycin Biosynthesis Revealing Unprecedented Architectural Complexity for a Hybrid Polyketide Synthase and Nonribosomal Peptide Synthetase. *Chem. Biol.* **11**, 33–45 (2004).

47. A. E. Fraley, M. Dell, M. Schmalhofer, R. A. Meoded, C. Bergande, M. Groll, J. Piel, Heterocomplex structure of a polyketide synthase component involved in modular backbone halogenation. *Structure*. **31**, 565–572.e4 (2023).

48. J. Moldenhauer, X.-H. H. Chen, R. Borriss, J. Piel, Biosynthesis of the Antibiotic Bacillaene, the Product of a Giant Polyketide Synthase Complex of the trans-AT Family. *Angew. Chem. Int. Ed.* **46**, 8195–8197 (2007).

49. C. Kohlhaas, M. Jenner, A. Kampa, G. S. Briggs, J. P. Afonso, J. Piel, N. J. Oldham, Amino acid-accepting ketosynthase domain from a trans-AT polyketide synthase exhibits high selectivity for predicted intermediate. *Chem. Sci.* **4**, 3212 (2013).

50. J. R. Lohman, M. Ma, J. Osipiuk, B. Nocek, Y. Kim, C. Chang, M. Cuff, J. Mack, L. Bigelow, H. Li, M. Endres, G. Babnigg, A. Joachimiak, G. N. Phillips, B. Shen, Structural and evolutionary relationships of "AT-less" type I polyketide synthase ketosynthases. *Proc. Natl. Acad. Sci.* **112**, 12693–12698 (2015).

51. R. Ueoka, A. Bhushan, S. I. Probst, W. M. Bray, R. S. Lokey, R. G. Linington, J. Piel, Genome-Based Identification of a Plant-Associated Marine Bacterium as a Rich Natural Product Source. *Angew. Chem. Int. Ed.* **57**, 14519–14523 (2018).

52. M. F. J. Mabesoone, S. Leopold-Messer, H. A. Minas, C. Chepkirui, P. Chawengrum, S. Reiter, R. A. Meoded, S. Wolff, F. Genz, N. Magnus, B. Piechulla, A. S. Walker, J. Piel, Evolution-guided engineering of trans-acyl transferase polyketide synthases - Zenodo repository 10.5281/zenodo.8146703.

53. R. C. Edgar, MUSCLE: a multiple sequence alignment method with reduced time and space complexity. *BMC Bioinformatics*. **5**, 113 (2004).

54. J. Jumper, R. Evans, A. Pritzel, T. Green, M. Figurnov, O. Ronneberger, K. Tunyasuvunakool, R. Bates, A. Žídek, A. Potapenko, A. Bridgland, C. Meyer, S. A. A. Kohl, A. J. Ballard, A. Cowie, B. Romera-Paredes, S. Nikolov, R. Jain, J. Adler, T. Back, S. Petersen, D. Reiman, E. Clancy, M. Zielinski, M. Steinegger, M. Pacholska, T. Berghammer, S. Bodenstein, D. Silver, O. Vinyals, A. W. Senior, K. Kavukcuoglu, P. Kohli, D. Hassabis, Highly accurate protein structure prediction with AlphaFold. *Nature*. **596**, 583–589 (2021).

55. M. A. Konkol, K. M. Blair, D. B. Kearns, Plasmid-Encoded ComI Inhibits Competence in the Ancestral 3610 Strain of Bacillus subtilis. *J. Bacteriol.* **195**, 4085–4093 (2013).

56. C. Engler, S. Marillonnet, "Generation of Families of Construct Variants Using Golden Gate Shuffling" in *cDNA Libraries* (Chaofu Lu,., 2011), pp. 167–181.

57. T. Cermak, E. L. Doyle, M. Christian, L. Wang, Y. Zhang, C. Schmidt, J. A. Baller, N. V. Somia, A. J. Bogdanove, D. F. Voytas, Efficient design and assembly of custom TALEN and other TAL effector-based constructs for DNA targeting. *Nucleic Acids Res.* **39**, e82–e82 (2011).

58. A. Loeschcke, A. Markert, S. Wilhelm, A. Wirtz, F. Rosenau, K.-E. Jaeger, T. Drepper, TREX: A Universal Tool for the Transfer and Expression of Biosynthetic Pathways in Bacteria. *ACS Synth. Biol.* **2**, 22–33 (2013).

59. D. Domik, A. Thürmer, T. Weise, W. Brandt, R. Daniel, B. Piechulla, A Terpene Synthase Is Involved in the Synthesis of the Volatile Organic Compound Sodorifen of Serratia plymuthica 4Rx13. *Front. Microbiol.* **7** (2016), doi:10.3389/fmicb.2016.00737.

60. R. Ueoka, A. Bhushan, S. I. Probst, W. M. Bray, R. S. Lokey, R. G. Linington, J. Piel, Genome-Based Identification of a Plant-Associated Marine Bacterium as a Rich Natural Product Source. *Angew. Chem. Int. Ed.* **57**, 14519–14523 (2018).

61. M. Rust, E. J. N. Helfrich, M. F. Freeman, P. Nanudorn, C. M. Field, C. Rückert, T. Kündig, M. J. Page, V. L. Webb, J. Kalinowski, S. Sunagawa, J. Piel, A multiproducer microbiome generates

chemical diversity in the marine sponge Mycale hentscheli. *Proc. Natl. Acad. Sci.* **117**, 9508–9518 (2020).

62. H. Wang, Z. Li, R. Jia, J. Yin, A. Li, L. Xia, Y. Yin, R. Müller, J. Fu, A. F. Stewart, Y. Zhang, ExoCET: exonuclease in vitro assembly combined with RecET recombination for highly efficient direct DNA cloning from complex genomes. *Nucleic Acids Res.* **46**, e28–e28 (2018).

63. D. G. Gibson, L. Young, R.-Y. Chuang, J. C. Venter, C. A. Hutchison, H. O. Smith, Enzymatic assembly of DNA molecules up to several hundred kilobases. *Nat. Methods*. **6**, 343–345 (2009).

64. S. Thoma, M. Schobert, An improved Escherichia coli donor strain for diparental mating. *FEMS Microbiol. Lett.* **294**, 127–132 (2009).

65. M. N. Price, P. S. Dehal, A. P. Arkin, FastTree 2 – Approximately Maximum-Likelihood Trees for Large Alignments. *PLoS One*. **5**, e9490 (2010).

66. G. E. Crooks, G. Hon, J.-M. Chandonia, S. E. Brenner, WebLogo: A Sequence Logo Generator. *Genome Res.* **14**, 1188–1190 (2004).

67. F. Sievers, A. Wilm, D. Dineen, T. J. Gibson, K. Karplus, W. Li, R. Lopez, H. McWilliam, M. Remmert, J. Söding, J. D. Thompson, D. G. Higgins, Fast, scalable generation of high-quality protein multiple sequence alignments using Clustal Omega. *Mol. Syst. Biol.* **7**, 539 (2011).

68. F. Sievers, D. G. Higgins, "The Clustal Omega Multiple Alignment Package" in *Multiple Sequence Alignment*, K. Katoh, Ed. (2021), pp. 3–16.

69. B. Wang, Y. Song, M. Luo, Q. Chen, J. Ma, H. Huang, J. Ju, Biosynthesis of 9-Methylstreptimidone Involves a New Decarboxylative Step for Polyketide Terminal Diene Formation. *Org. Lett.* **15**, 1278–1281 (2013).

70. R. Sigrist, H. Luhavaya, S. M. K. McKinnie, A. Ferreira da Silva, I. D. Jurberg, B. S. Moore, L. Gonzaga de Oliveira, Nonlinear Biosynthetic Assembly of Alpiniamide by a Hybrid cis/trans-AT PKS-NRPS. *ACS Chem. Biol.* **15**, 1067–1077 (2020).

71. C. Paulus, Y. Rebets, J. Zapp, C. Rückert, J. Kalinowski, A. Luzhetskyy, New Alpiniamides From Streptomyces sp. IB2014/011-12 Assembled by an Unusual Hybrid Non-ribosomal Peptide Synthetase Trans-AT Polyketide Synthase Enzyme. *Front. Microbiol.* **9** (2018), doi:10.3389/fmicb.2018.01959.

72. S. Alt, B. Wilkinson, Biosynthesis of the Novel Macrolide Antibiotic Anthracimycin. *ACS Chem. Biol.* **10**, 2468–2479 (2015).

73. K. Jungmann, R. Jansen, K. Gerth, V. Huch, D. Krug, W. Fenical, R. Müller, Two of a Kind—The Biosynthetic Pathways of Chlorotonil and Anthracimycin. *ACS Chem. Biol.* **10**, 2480–2490 (2015).

74. T. M. Nye, J. W. Schroeder, D. B. Kearns, L. A. Simmons, Complete Genome Sequence of Undomesticated Bacillus subtilis Strain NCIB 3610. *Genome Announc.* **5** (2017), doi:10.1128/genomeA.00364-17.

75. M. J. Bertin, A. Vulpanovici, E. A. Monroe, A. Korobeynikov, D. H. Sherman, L. Gerwick, W. H. Gerwick, The Phormidolide Biosynthetic Gene Cluster: A trans-AT PKS Pathway Encoding a Toxic Macrocyclic Polyketide. *ChemBioChem*. **17**, 164–173 (2016).

76. A. Nakabachi, R. Ueoka, K. Oshima, R. Teta, A. Mangoni, M. Gurgui, N. J. Oldham, G. van Echten-Deckert, K. Okamura, K. Yamamoto, H. Inoue, M. Ohkuma, Y. Hongoh, S. Miyagishima, M. Hattori, J. Piel, T. Fukatsu, Defensive Bacteriome Symbiont with a Drastically Reduced Genome. *Curr. Biol.* **23**, 1478–1484 (2013).

77. K. P. Yuet, C. W. Liu, S. R. Lynch, J. Kuo, W. Michaels, R. B. Lee, A. E. McShane, B. L. Zhong, C. R. Fischer, C. Khosla, Complete Reconstitution and Deorphanization of the 3 MDa Nocardiosis-Associated Polyketide Synthase. *J. Am. Chem. Soc.* **142**, 5952–5957 (2020).

78. M. A. Storey, S. K. Andreassend, J. Bracegirdle, A. Brown, R. A. Keyzers, D. F. Ackerley, P. T. Northcote, J. G. Owen, Metagenomic Exploration of the Marine Sponge Mycale hentscheli Uncovers Multiple Polyketide-Producing Bacterial Symbionts. *MBio*. **11** (2020), doi:10.1128/mBio.02997-19.

79. Y. Zou, H. Yin, D. Kong, Z. Deng, S. Lin, A Trans-Acting Ketoreductase in Biosynthesis of a Symmetric Polyketide Dimer SIA7248. *ChemBioChem*. **14**, 679–683 (2013).

80. M. Steinmetz, R. Richter, Easy cloning of mini-Tn10 insertions from the Bacillus subtilis chromosome. *J. Bacteriol.* **176**, 1761–1763 (1994).

81. X. Yan, H.-J. Yu, Q. Hong, S.-P. Li, Cre/ lox System and PCR-Based Genome Engineering in Bacillus subtilis. *Appl. Environ. Microbiol.* **74**, 5556–5562 (2008).

82. J. Moldenhauer, D. C. G. Götz, C. R. Albert, S. K. Bischof, K. Schneider, R. D. Süssmuth, M. Engeser, H. Gross, G. Bringmann, J. Piel, The Final Steps of Bacillaene Biosynthesis in Bacillus amyloliquefaciens FZB42: Direct Evidence for β,γ Dehydration by a trans-Acyltransferase Polyketide Synthase. *Angew. Chem. Int. Ed.* **49**, 1465–1467 (2010).

Captions

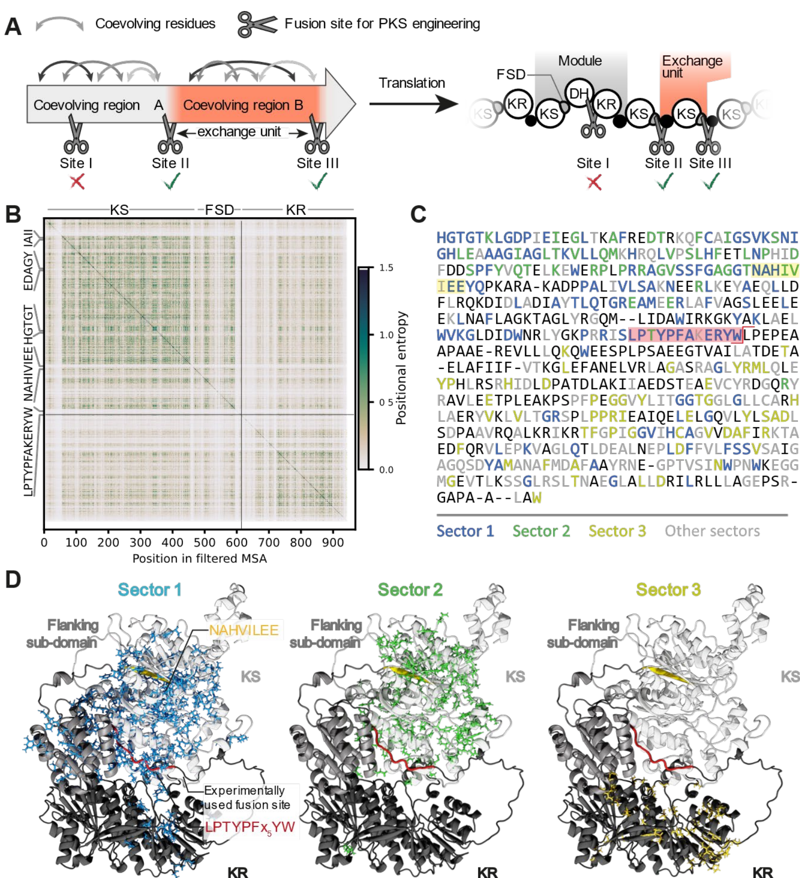

Figure 1. SCA identifies the LPTYPFx$_5$W motif as a candidate fusion point for chimeric *trans*-AT PKSs. (**A**) Engineering within regions of coevolving residues is hypothesized to perturb important amino acid interactions, yielding non-functional chimeras (site I). In contrast, engineering at boundaries between regions of coevolving residues minimizes such perturbations and might lead to functional chimeras (sites II and III). At the protein level, *trans*-AT PKS exchange units span between the C-terminal boundaries of the FSDs, which slightly contrasts with the commonly used PKS module boundaries, spanning from KS to ACP. (**B**) Covariance matrix of Clustal-aligned (*53*) multiple sequence alignments of the KS-FSD-KR tridomain, showing the positional entropy obtained from SCA for amino acid residue pairs of the tridomain. The position of conserved IAII, HGTGT, NAHVILEE, and LPTYPFx$_5$W motifs are indicated on the side. (**C**) Consensus sequence of the C-terminal part of the KS-FSD-KR tridomain obtained from the conservation-filtered sequence alignment used for SCA. Residues are color-coded according to SCA sectors. Residues not assigned to sectors are black. The NAHVILEE motif and the experimentally used engineering site downstream of the LPTYPFx$_5$W motif is indicated with the yellow and red shades, respectively. (**D**) 3D visualizations of sector 1 (left), sector 2 (middle), and sector 3 (right) on an alphaFold2-generated (*54*) model of the OocR KS-FSD-KR tridomain. Colors correspond to residue colors in panel B.

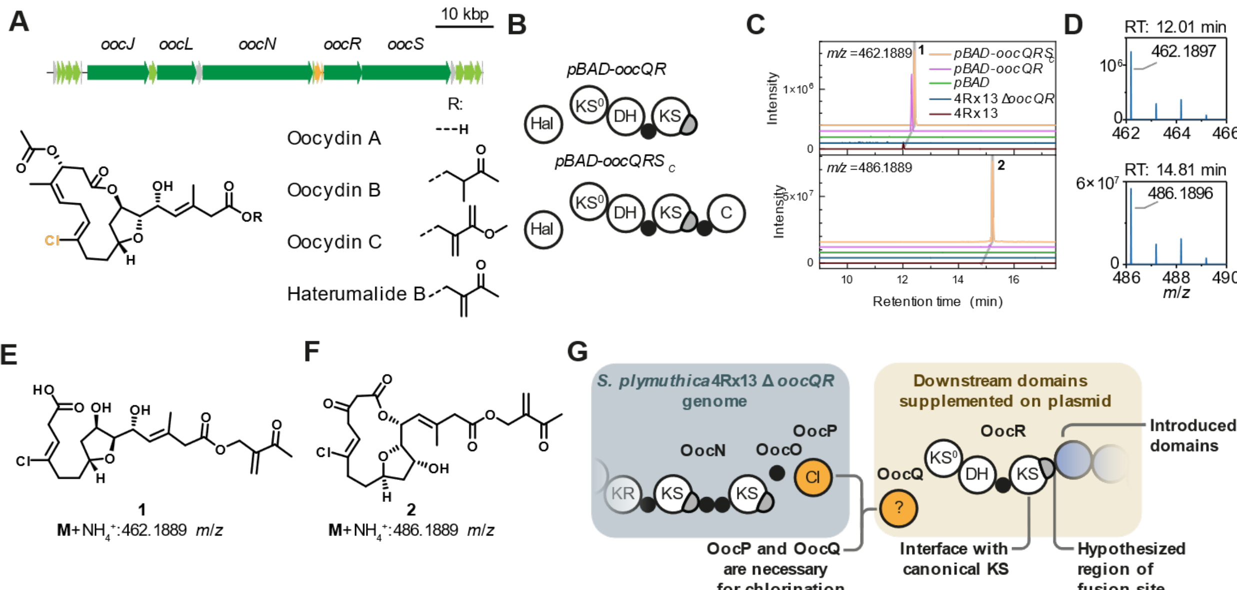

Figure 2 The oocydin BGC as platform for PKS engineering. (**A**) The oocydin BGC from *S. plymuthica* 4Rx13 and chemical structures of natural oocydin congeners. Core PKS genes are shaded dark green, accessory biosynthetic genes light green, *oocP* and *oocQ* are shaded yellow. (**B**) Domain motifs of truncated OocR PKSs and OocQ as supplemented with the *pBAD-oocQR* and *pBAD-oocQRS$_C$* plasmids. (**C**) EICs for **1**+NH_4^+ (top) and **2**+NH_4^+ (bottom) for *S. plymuthica*, *S. plymuthica* Δ*oocQR* and *S. plymuthica* Δ*oocQR* supplemented empty *pBAD*, *pBAD-oocQR* and *pBAD-oocQRS$_C$* plasmids. (**D**) Isotope patterns confirm chlorination of **1** (top) and **2** (bottom). (**E**) Putative chemical structures of **1** and (**F**) NMR-confirmed structure of **2**. (**G**) The engineering strategy relies on supplementing *oocQ* and engineered variants of *oocR* on a *pBAD* plasmid.

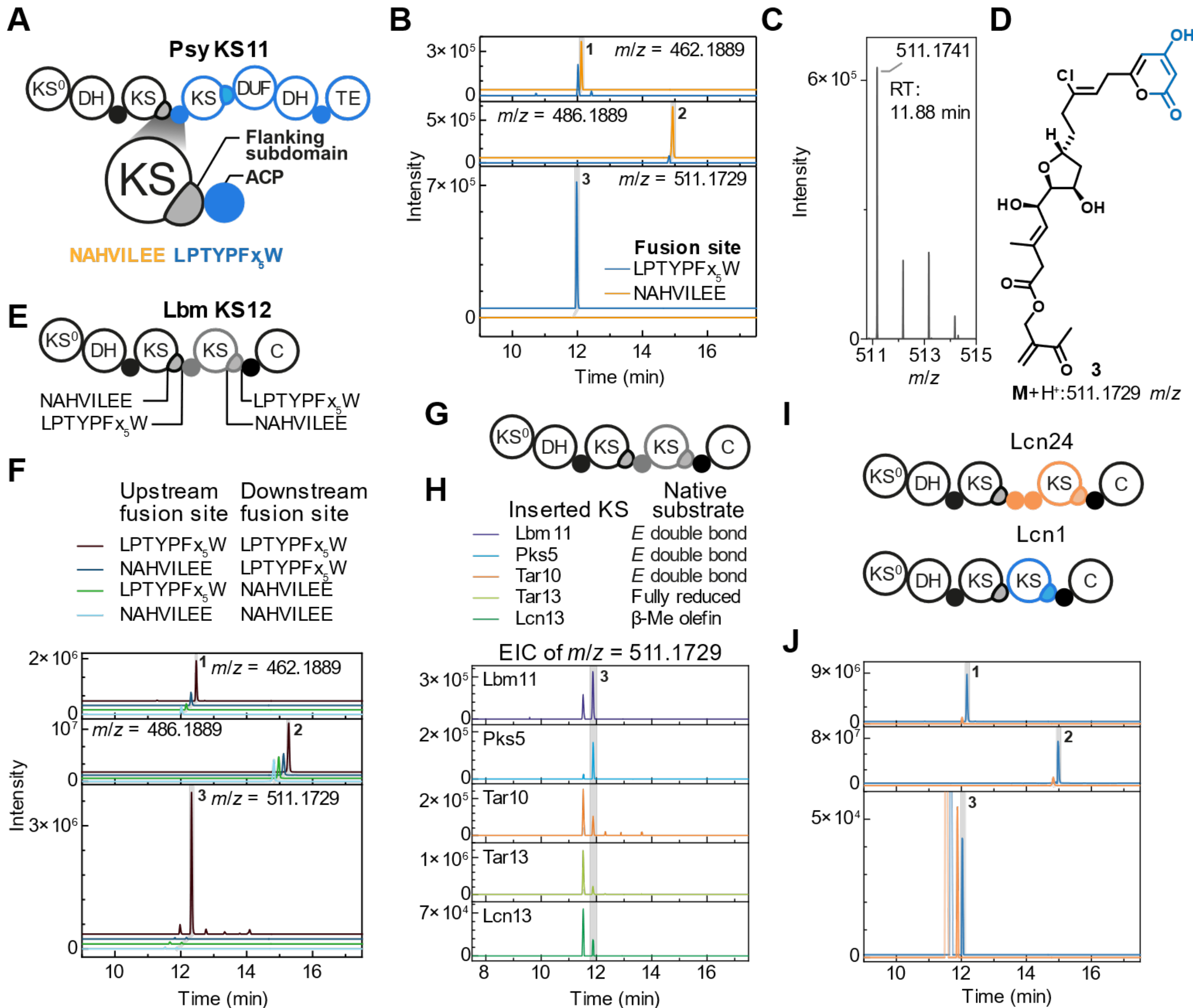

Figure 3 Insertion of KS domains yields various functional chimeric PKSs. (**A**) Domain architecture of chimeric PKSs incorporating the terminal domains of the psymberin (*psy*) PKS. The two fusion sites are indicated in the enlarged region. (**B**) Extracted ion chromatograms (EIC)s for **1**, **2**, and **3** from mutant cultures harboring the *ooc-psy* chimeras. (**C**) Mass spectrum of **3** at a retention time of 11.88 min showing the characteristic peak pattern indicative of chlorination. (**D**) NMR-characterized structure of **3**. (**E**) Domain architecture of the various chimeric PKSs incorporating lobatamide (*lbm*) KS12 with its native upstream ACP. The two fusion sites upstream and downstream of the inserted ACP-KS domain series are indicated. (**F**) EICs for **1**, **2**, and **3** from mutant cultures harboring the *ooc-lbm-ooc* chimeras. (**G**) Domain architecture of additional chimeric PKSs incorporating ACP-KS domain series with various foreign non-matching KSs, i.e., which naturally accept substrates other than β-ketoacyl thioesters. (**H**) EICs for **3** of mutant cultures harboring these chimeric PKSs. (**I**) Domain architecture of the two chimeric PKSs incorporating ACP-KS domain series from N-termini of PKS proteins. (**J**) EICs for **1**, **2**, and **3** from mutant cultures harboring the chimeric PKSs. The peak eluting at 11.51 minutes originating from a prematurely offloaded intermediate has been blurred. See Fig. S16 for additional details.

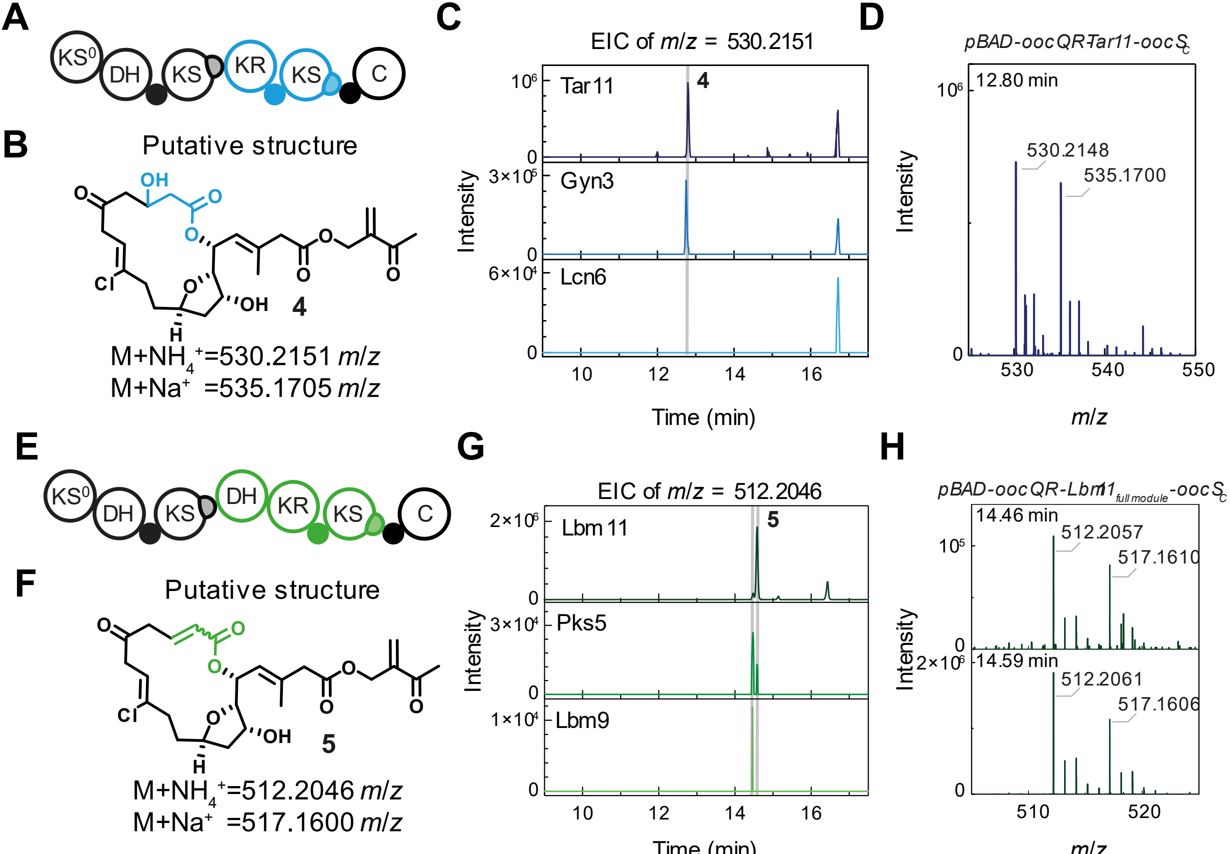

Figure 4 Domain series with additional modifying domains can be engineered into chimeric PKSs. (**A**) Domain architecture of the chimeric PKS incorporating reducing domain series. (**B**) Putative structure of hydroxylated polyketide **4**. (**C**) EICs for *m/z*=530.2151 of extracts of cultures of mutants expressing chimeric, reducing PKSs. The peak assigned to **4** is indicated by the shaded area. (**D**) Mass spectrum of the peak eluting at 12.80 minutes from culture extracts of *S. plymuthica pBAD-oocQR-tar11-oocS$_C$*, showing masses and chlorination isotopes patterns corresponding to NH_4^+ and Na^+ adducts of **4**. (**E**) Domain architecture of the chimeric PKS incorporating dehydrating domain series. (**F**) Putative structure of dehydrated polyketide **5**. (**G**) EICs for *m/z*=512.2046 of extracts of cultures of mutants expressing chimeric, dehydrating PKSs. (**H**) Mass spectra of the peaks eluting at 14.46 and 14.59 minutes from culture extracts of *S. plymuthica pBAD-oocQR-lbm11$_{DH\text{-}KR\text{-}ACP\text{-}KS}$-oocS$_C$*, showing masses and chlorination isotopes patterns corresponding to NH_4^+ and Na^+ adducts of **5**.

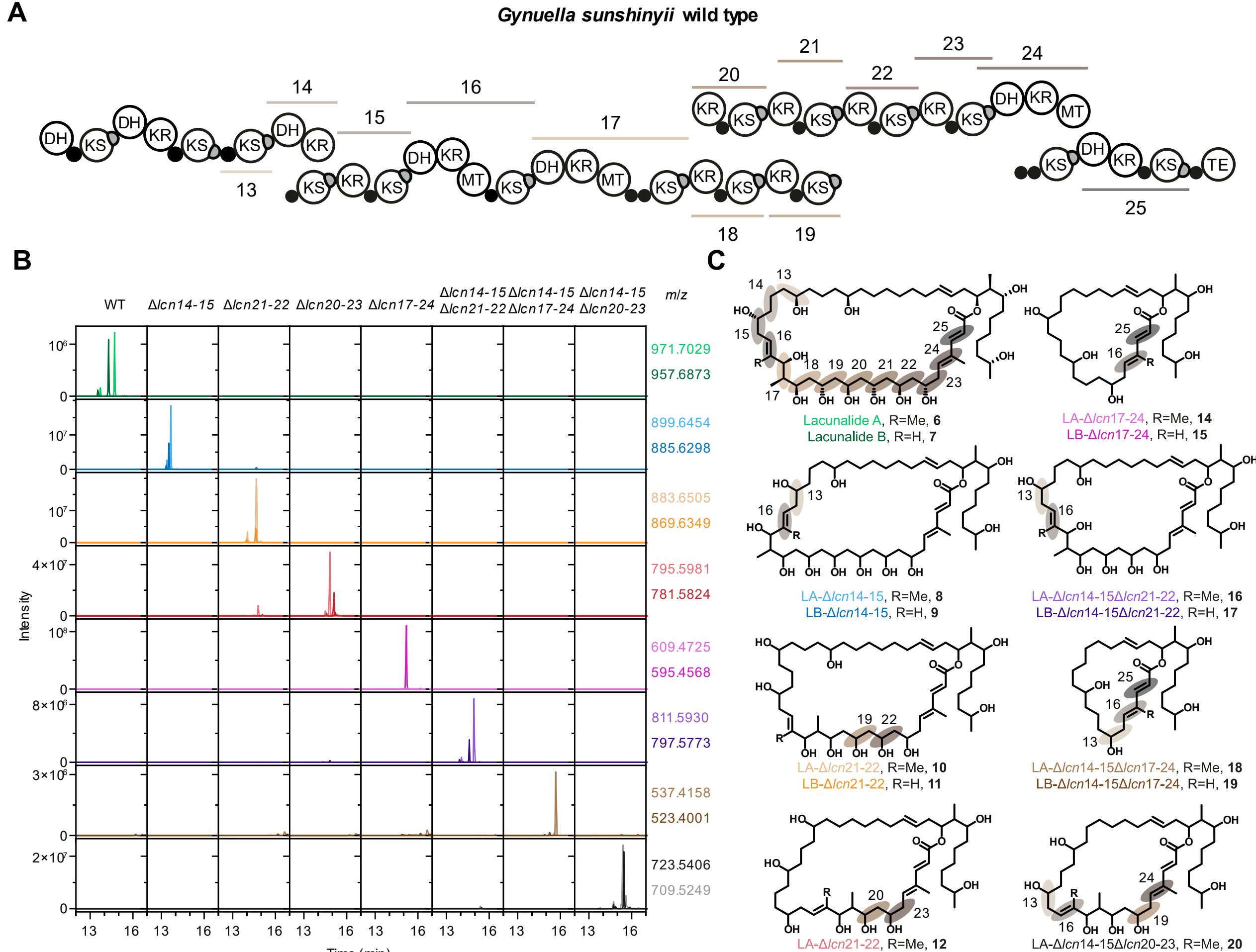

Figure 5 The engineering strategy enables biosynthesis of truncated lacunalides. (**A**) The domain architecture of the last PKSs in the lacunalide (*lcn*) PKS in wild type (WT) *G. sunshinyii* YC6258. (**B**) EICs for *m/z* values corresponding to proton adducts of compounds **6**-**21** for the various *G. sunshinyii* mutants. Each column shows the EICs obtained for the mutant mentioned above the column. The rows show the EICs obtained for *m/z* values indicated at the right of the row. Masses corresponding to **15** and **19** could not be observed. (**C**) Chemical structures of wild-type lacunalide A (**6**), lacunalide B (**7**), the NMR-confirmed truncated lacunalides **8**,**9**, **10**, **11**, **12**, **14**, **16**, **18**, **20**, and **21** and putative structures of truncated lacunalides **13** and **17**. The shaded numbered circles indicate the moieties installed by the corresponding *lcn* domain series.